

UNCLASSIFIED

Defense Technical Information Center  
Compilation Part Notice

ADP020046

TITLE: Porcine Skin Thermal Response to Near-IR Lasers Using a Fast Infrared Camera

DISTRIBUTION: Approved for public release, distribution unlimited

This paper is part of the following report:

TITLE: Laser Interaction with Tissue and Cells XV. Held in San Jose, Ca on 26-28 January 2004.

To order the complete compilation report, use: ADA436676

The component part is provided here to allow users access to individually authored sections of proceedings, annals, symposia, etc. However, the component should be considered within the context of the overall compilation report and not as a stand-alone technical report.

The following component part numbers comprise the compilation report:

ADP020007 thru ADP020056

UNCLASSIFIED

# Porcine skin thermal response to near-IR lasers using a fast infrared camera

Clarence Cain<sup>1</sup>, Thomas Milner<sup>2</sup>, Sergey Telenkov<sup>2</sup>, Kurt Schuster<sup>1</sup>,  
Kevin Stockton<sup>1</sup>, David Stolarski<sup>1</sup>, Chris Condit<sup>2</sup>, Ben Rockwell<sup>3</sup>,  
William Roach<sup>3</sup> and A. J. Welch<sup>2</sup>

<sup>1</sup>Northrop Grumman IT, 4241 Woodcock Dr., Suite B-100, San Antonio, TX 78228

<sup>2</sup>University of Texas, Biomedical Engineering Department, Austin, Texas 78712

<sup>3</sup>U.S. Air Force Research Laboratory, HEDO, Brooks City-Base, TX 78235-5278

## ABSTRACT

We have measured the minimum visible lesion (MVL) thresholds for porcine skin and determined the ED<sub>50</sub> for exposures at 1314 nm for 0.35 ms laser pulses. An *in-vivo* pigmented animal model, Yucatan mini-pig (*Sus scrofa domestica*), was used in this study. We also have measured the 2-D thermal response using a high-speed (100 frames per second) infrared camera for single-pulse temperature recordings for Gaussian beams of 1 mm diameter. *In Vitro* samples of the same pig skin were used for measurements of the optical properties (absorption coefficient,  $\mu_a$ , and reduced scattering coefficient  $\mu_s$ ) as a function of wavelength around 1315 nm wavelength. A measured surface temperature distribution for one IR laser pulse of 0.37J at a spot size of 1.3 mm diameter gave approximately a 43° C rise at a hot spot. Computed temperature distributions as a function of time and space are presented and compared with the measured surface temperatures.

**Key Words:** laser, skin, mini-pig, porcine, infrared, temperature, thermal, MVL

## 1. INTRODUCTION

Different types of lasers are being operated for everyday uses and more are being developed yearly. Many of these lasers have not been characterized as to their capability of doing damage to biological systems such as the eye or skin. Much more research has been accomplished to determine the damage mechanisms and levels of exposure causing damage to the eye than to skin. Skin effects are now being studied because the increasing threat posed by a new generation of extremely high energy level near-infrared (NIR) lasers. These lasers are becoming increasingly popular in various industrial applications and they are being studied for their threat level. The ANSI standard Z136.1, 2000<sup>1</sup> defines wavelengths in the range of 1200 nm to 1400 nm to be NIR and specifies a constant maximum permissible exposure (MPE) for skin for these wavelengths.

Data and pictures presented herein were obtained during the visible lesion threshold study using a common laser that generates these wavelengths (1315 nm) at energies from millijoules to joules. The neodymium:ytterbium-lithium-fluoride (Nd:YLF) laser actually produces a wavelength of 1314 nm, but can be shifted in frequency and wavelength by several methods. There are also other high-energy lasers operating at this wavelength such as the Chemical-Oxygen-Iodide-Laser (COIL). The data presented in this study was produced using a single pulse Nd:YLF laser system in the long pulse mode (350  $\mu$ s).

The ANSI Z136.1 Sub-Committee establishes MPE levels using threshold studies, and there has been much work researching the ocular effects of this wavelength region<sup>2,3,4</sup>, but little for skin effects. Therefore the skin MPE levels have been based on sparse experimental data for skin exposures in the visible or near-IR. The data on porcine skin damage thresholds obtained from this study will contribute to the further understanding of laser injury mechanisms and will add to the existing data on laser skin effects, on which safety standards are based and which affect employment of these laser systems. This study uses the Yucatan mini-pig (*Sus scrofa domestica*) as the model in animal use studies to determine the estimated dose for 50% probability of laser-induced damage (ED<sub>50</sub>) for laser injury to skin at 1314nm wavelength for a single 0.35ms pulse duration exposure.

This research included multiple tasks covering mathematical modeling of laser/tissue interactions and measurements of skin temperature increase due to near-IR laser pulses recorded by a high-speed, near-IR camera that was operated at a 100 frames per second. The Takatas Skin Model<sup>5</sup> presently being used was developed over 30 years ago and does not account for the present-day understanding of the effects of scattering on light propagation in tissue. The Takata Model does not account for the absorption of photons beyond the beam, backscattering of light and effective attenuation of the attenuated light with depth that is a function of local absorption, scattering and phase functions. The newer Monte Carlo Simulation Model<sup>6</sup> does include scattering and requires a scattering coefficient to quantify the heat source terms due to the laser light entering the tissue. Prediction of temperature rises and damage levels by the two models were to be compared using their respective input parameters. These parameters were measured by University of Texas at Austin, Biomedical Engineering Department, for porcine skin.

## 2. METHODOLOGY

*In vivo* temperature profiles in space and in time were recorded and compared with predicted skin-temperature increases by the Takata Skin Model and a combined Monte Carlo optical model and finite element thermal model. The Takata Skin Model was run using old and new parameters for porcine skin samples and the Monte Carlo finite element (FE) Model was used as a comparison model. Data was compared between models and with actual temperature measurements in the lab and with the damage thresholds previously measured by in our laboratory. Prior to the modeling, skin samples from a porcine subject were used for the measurement of absorption and

scattering coefficients for wavelengths between 1 and 2 microns, especially at 1.314 and 1.54 microns. These measurements were made to provide reliable input parameters for both the Takata Model and the Monte Carlo/FE Skin Model.

Laser exposures were accomplished with a laser system (Positive Light), using a Nd:YLF rod, delivering 1314 nm light at 0.350ms exposure time, and at various pulse energies. The laser produced a top-hat profile, and two experimental spot sizes (700 microns and 1300 microns) were used in this study. Spot sizes were measured using an Electro Physics IR camera with a Spiricon LBA 500 Laser Beam analyzer and beam grabber card. The pulse duration was measured by an ET-3000 InGaAs Electro-Optics Technology, Inc. photodiode connected to a Tektronix TDS 220 oscilloscope. Energy measurements were made with a Molectron EPM2000 energy meter and JD25 and JD50 energy probes, which were placed after a 90/10 beam splitter to collect 10% of the beam energy, and thus determine the actual energy delivered to the skin. An articulating arm laser beam delivery system from Laser Mechanisms, Inc, was used to deliver the beam without having to move the subject. A metal "aiming ring" was attached to the end of the articulating arm, which maintained a constant distance between the arm's aperture and the target area of the skin. This provided the precise positioning and distance control necessary to deliver exposures of known spot-size, more accurate beam delivery and a higher number of exposures per subject, resulting in a reduction of the total number of subjects required. The laser system setup is depicted in Figure 1.

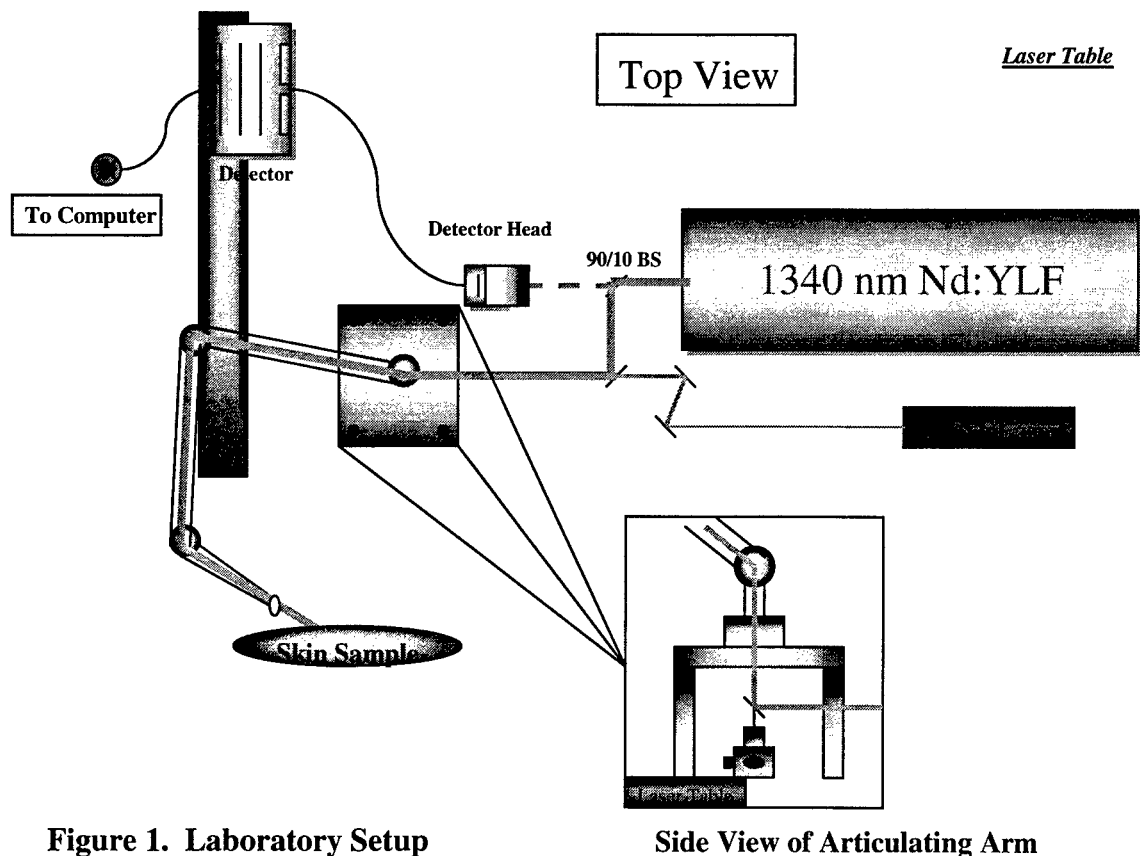


Figure 1. Laboratory Setup

Side View of Articulating Arm

Measurements of laser-induced temperature increase in porcine skin samples were carried out using high-speed IR focal plane array (FPA) camera sensitive in the mid-infrared (3 – 5  $\mu\text{m}$ ) spectral band (Phoenix model, Indigo Systems, Santa Barbara, CA). To acquire reference IR image frames prior to laser exposure, the IR camera was operating in free running mode at frame rate of 100 Hz and the image size of 256x256 pixels. The IR camera lens was extended to provide spatial resolution approximately 30  $\mu\text{m}/\text{pixel}$  of two-dimensional temperature distribution at the laser spot on skin surface. In our experiments, image acquisition was triggered 650 ms prior to laser exposure and sequence of 500 frames was recorded to investigate laser-induced temperature increase. Because IR image acquisition was not synchronized with pulsed laser exposure, there was uncertainty less than 10 ms in temporal position of the peak temperature recorded by the IR camera. However, due to relatively low thermal diffusivity of tissue, temperature change during the 10 ms time interval is negligible and can be ignored.

The Yucatan mini-pig model (Lonestar Laboratory Swine, Seguin, TX) was selected since it is more similar to human skin than the commonly used Yorkshire model<sup>7</sup>. Yucatan mini-pig skin is melanated and, on the flank, is of similar thickness to that on the human arm, which has high probability of accidental exposure. By using this model, the properties of human skin can be more closely approximated to gain a better understanding of the human laser tissue interaction for the wavelength of interest.

Six female Yucatan mini-pigs weighing between 25 and 40 kg were involved in this study. Five separate flanks were used at each spot size. The animals were between 3 and 8 months of age. All procedures followed an approved Animal Use Protocol using routine procedures in order to maximize the results from a limited number of subjects. The animals involved in this study were procured, maintained, and used in accordance with the Federal Animal Welfare Act and the "Guide for the Care and Use of Laboratory Animals" prepared by the Institute of Laboratory Animal Resources -- National Research Council. Brooks City-Base, TX has been fully accredited by the Association for Assessment and Accreditation of Laboratory Animal Care, International (AAALAC) since 1967.

One animal was euthanized after exposure to provide skin samples for the absorption and scattering parameter measurements. Skin samples were taken from each flank after experimental temperature measurements were accomplished. The other five were part of an animal-sharing program. All pigs were fed standard, commercially available diets, and had unlimited access to water. However, solid food was withheld for 12 hours prior to laser exposure and biopsy collection.

The pigs were sedated by single syringe injection of Tiletamine/Zolazepam (4-6 mg/kg) intramuscular (IM) and Xylazine (2.2 mg/kg) IM, and maintained on inhalation isoflurane anesthesia during all procedures. After sedation, hair on the flank was clipped using hand clippers, and the cleansed skin was inspected by each of three evaluators to check for redness, irritation or other confounding marks. Physiological parameters were monitored throughout all procedures. Buprenorphine (0.05-0.1 mg/kg) was administered

intramuscularly for analgesia after biopsies were complete. The animals were returned to their runs upon recovery to sternal recumbency from anesthesia.

Target areas were marked with two 6 cm x 6 cm grids with a permanent-ink marker making a total of 72 grid squares per flank. As previously mentioned, the distance between the articulating arm aperture and the skin was kept constant by the use of a metal device attached to the end of the arm. Once the animal was positioned on a table, it was not moved during procedures. Energy was delivered randomly to one grid at systematically varied intensities, and this process was then repeated on the second grid.

Visual evaluation of skin exposure sites was performed immediately after exposures of a grid. The grid was re-examined at one-hour and 24 hours post exposure. Three trained lesion readers were used to evaluate the presence or absence of skin lesions. The readers used a lighted magnifying glass to examine the exposed skin area. The three readers independently examined the flank lesions immediately after all 72 exposures were accomplished. A lesion was recorded as a "yes" if at least two readers identified it as positive. Then, one control biopsy was taken from flank skin located outside the exposure grids. The exposure grids were re-examined in the same way at 1 hour and at 24 hours post-exposure, and two full-thickness biopsy specimens were taken at each time from sites that showed lesions. Biopsy skin samples were taken using a 6-mm skin biopsy punch, and immediately closed with a non-absorbable suture, then topically medicated with Trio-mycin ointment. Harvested tissue was prepared for histopathologic analysis using 10% formalin solution, then blocked in paraffin and stained with hematoxylin/eosin (H&E). An Olympus Vanox-S camera was used to magnify, evaluate and photograph the samples.

Probit analysis<sup>8</sup> was the statistical method used to determine the estimated dose for 50% probability of laser-induced damage ( $ED_{50}$ ) for the *in-vivo* skin model. Data points were entered into the Probit statistical analysis package and the  $ED_{50}$  was calculated along with fiducial limits at the 95% confidence level. All results were then to be compared to each other for the predictability of temperature increases and damage

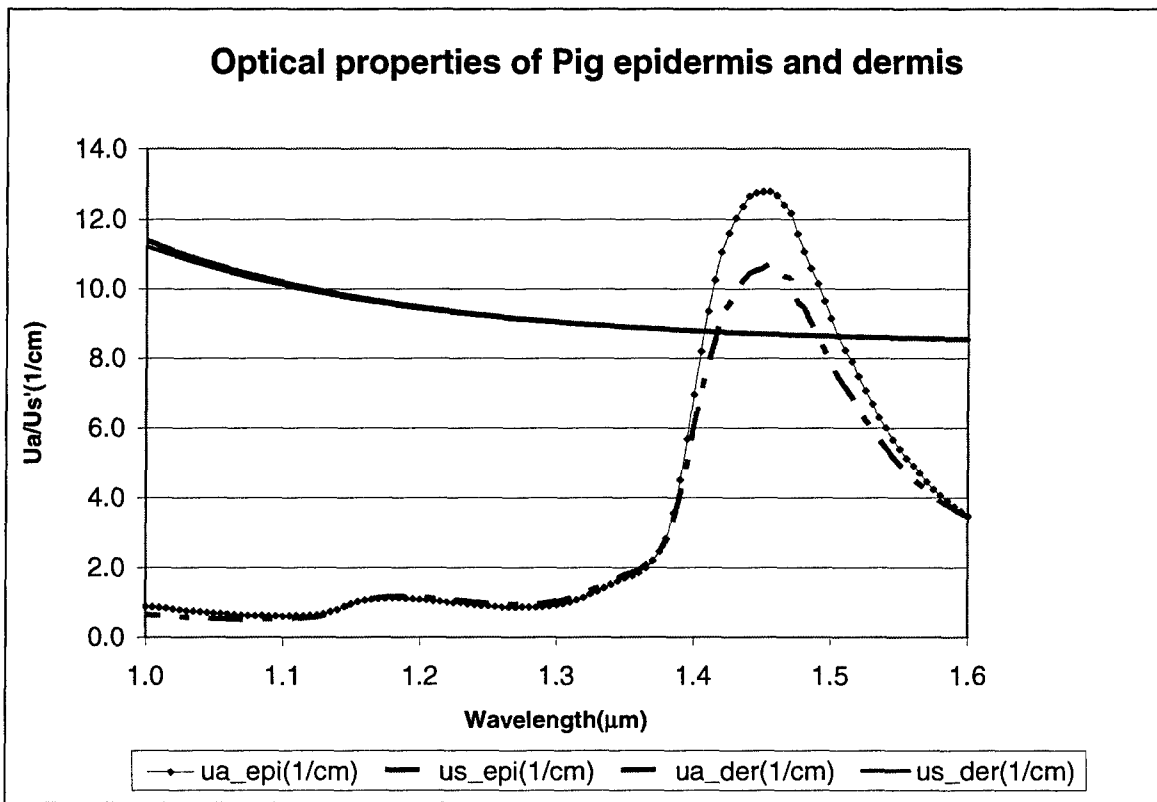
### 3. DATA AND RESULTS

Table 1 lists the measured values  $\mu_a$  and  $\mu_s'$  along with  $\mu_s$  calculated for an assumed value of  $g=0.9$  for the Yucatan mini-pig skin supplied by AFRL/HEDO. Skin samples were harvested immediately after the temperature rises were recorded by the high-speed IR camera and packed in ice for transportation to the University of Texas.

We measured the optical properties of the porcine skin as a function of wavelength and layer of skin and these are shown in Figure 2 for both the absorption parameter and scattering parameter. This figure gives four parameters, both absorption and reduced scattering coefficients, for the epidermis and dermal layer from 1  $\mu\text{m}$  out to 1.6  $\mu\text{m}$ .

ua(1/cm) = absorption coef. us(1/cm) = scattering coef. us'(1/cm) = reduced scattering					
Tissue (Pigmented Pig)	wave(nm)	ua(1/cm)	us(1/cm)	us'(1/cm)	g
epi_pig epi = epidermis,	1315	1.07	90.03	9.003	0.9
	1320	1.14	89.89	8.989	
	1540	6.00	86.02	8.602	
der_pig der = dermis	1315	1.19	89.77	8.977	0.9
	1320	1.25	89.63	8.963	
	1540	5.42	85.98	8.598	

Table 1. Optical properties of skin samples supplied by AFRL/HEDO and measured for Yucatan mini-pig epiderms and dermis



Note: Top two curves are for scattering and bottom two are for the absorption.

Figure 2.. Optical properties of pig epidermis and dermis for Yucatan minipig

Maximum temperature rise measured on the surface of the porcine skin as a function of laser pulse energies is shown in Figure 3 for a spot size of 0.7 mm diameter using the near-IR high speed camera operating at 100 frames per second. An ambient skin temperature of 27 °C was measured and this initial temperature is included in Figure 3. Figure 3 also shows the maximum measured temperature as a function of laser pulse energy together with the Monte Carlo/FE calculated temperature rises. Included in this figure is the predicted axial temperature by the Takata Model for energies out to 1.0 joule. There is a 10-ms uncertainty as to where the beginning of the temperature measurements

occurred since the IR camera was free-running at 100 frames/sec and was not synchronized with the beginning or ending of the laser pulse. This could account for some of the lower readings of the camera.

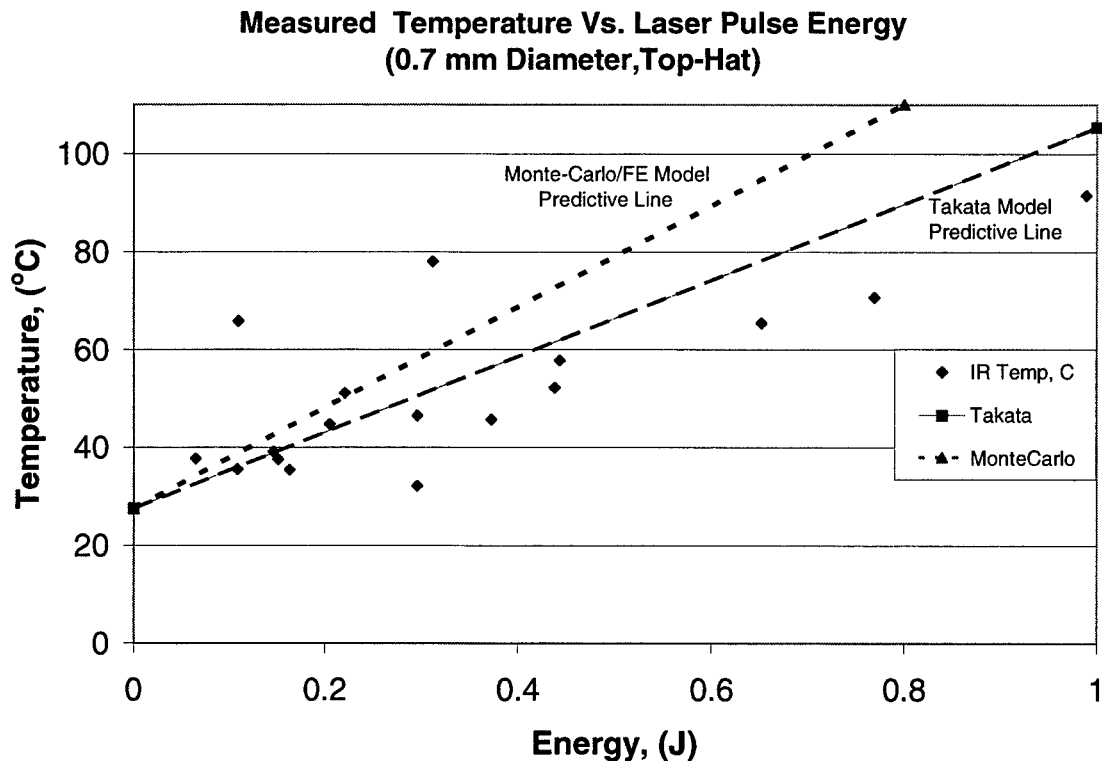


Figure 3. Measured and model predicted temperatures for a top-hat laser profile.  
Data points on axis are camera overloads and not real

Figure 4 is a graph of the temperature rises measured with the high-speed IR-camera for a larger spot size (1.3 mm flattop) and both model-calculated temperatures. This graph shows the calculated temperature increases by the Takata model for pulse energies up to 1.4 J and the Monte Carlo/FE Model for pulse energies up to 1.1 J, with all other values remaining the same as for Figure 3. Trend lines are added to show the linearly calculated temperatures as a function of pulse energy. Again, both models predict slightly higher temperature increases than measured by the IR camera, but as before, the model has not been validated using these new parameters.



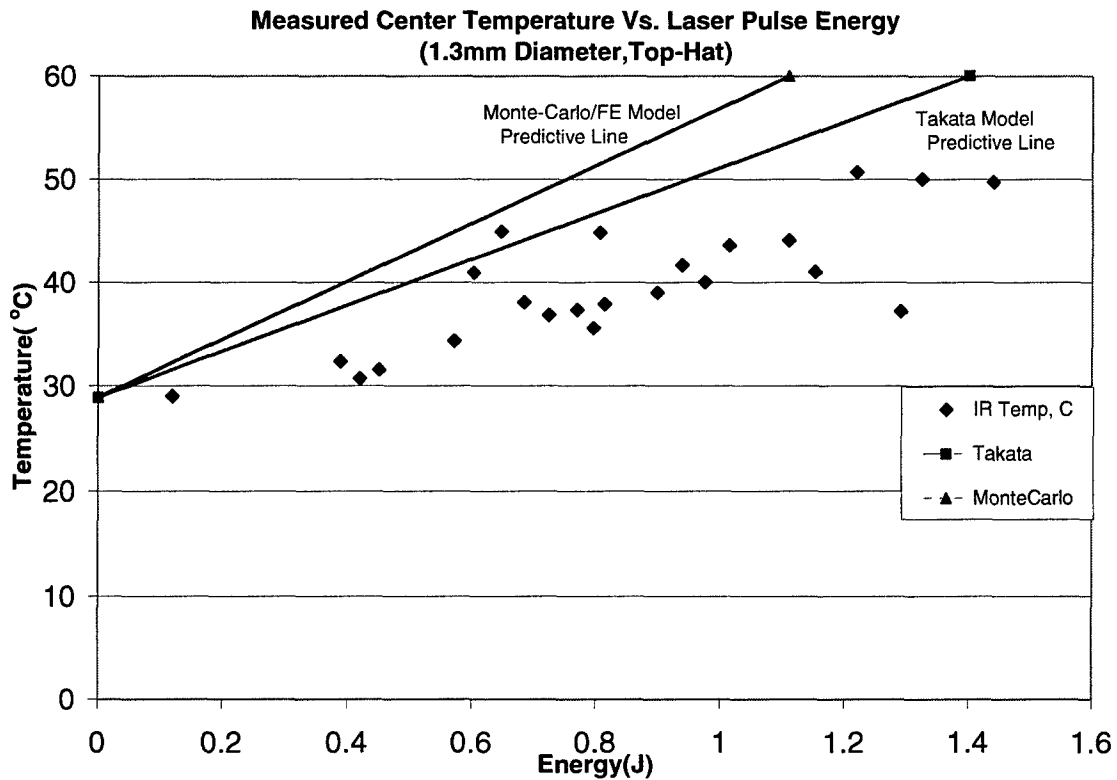


Figure 4. Measured and model predicted temperatures for a top-hat laser profile.

Figures 5 and 6 compare the calculated temperature profiles for the surface temperature distribution for both models using the MVL-ED<sub>50</sub> threshold energy levels for the top-hat laser profile. Figure 5 shows that there is only a 4 to 5 °C difference in calculated temperatures between the two models for the 0.7 mm diameter spot size. Figure 6 shows roughly the same temperature distributions for the 1.3 mm diameter beam and its respective MVL-ED<sub>50</sub> threshold energy. Since these are top-hat laser pulse profiles, the calculated temperatures drop off very rapidly outside of the beam diameter.

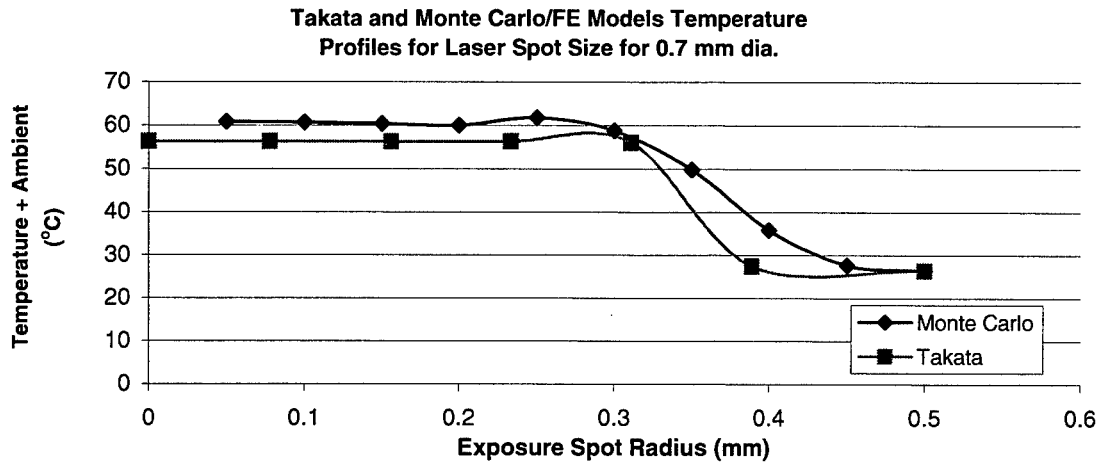


Figure 5. Takata and Monte Carlo/FE Model predicted temperatures versus a top-hat profile with a spot size of 0.7 mm in diameter.

The extent of irreversible damage is predicted using the same expression for each model that was originally proposed by Henriques<sup>9</sup> and subsequently used by a number of other investigators. Even though each model uses the same rate process equation, each produces different results because the users utilized different input parameters. The Takata model actually calculates five degrees of burn from 1<sup>st</sup> through 5<sup>th</sup> degree by specifying different levels of damage integral outputs for each degree. The Monte Carlo/FE model calculates the same damage integral output but does not associate a degree of burn with any level because originally this model only specified a burn/no-burn for the skin. This model could associate a degree of burn with a specified damage integral

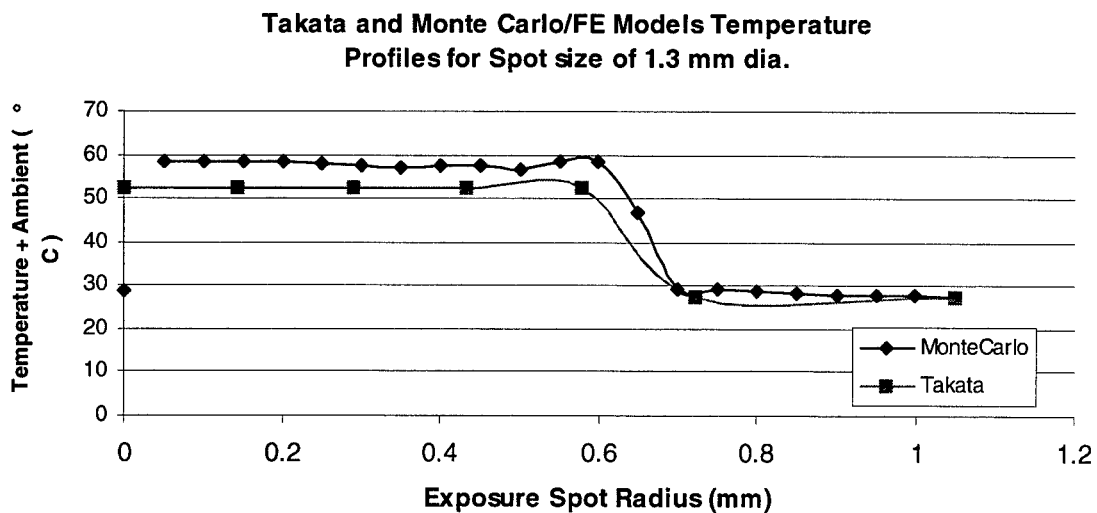


Figure 6 Takata and Monte Carlo/FE Model predicted temperatures versus a top-hat profile with a spot size of 1.3 mm in diameter

output value if desired. For instance, the Takata model calculated the burn level to be 2<sup>nd</sup> degree for the small diameter spot size, 0.7 mm, with damage integral output level being 6.5 for the highest temperature increase at the MVL-ED<sub>50</sub> threshold. The Monte Carlo/FE Model calculated the damage integral to be 588 at the end of the laser pulse and 1.7E+6 at the end of 5 seconds for the same MVL-ED<sub>50</sub> threshold energy. For the larger spot size and higher energy threshold at 1.3 mm diameter, Takata gives only a 1<sup>st</sup> degree burn with the output being 0.66 (2<sup>nd</sup> degree starts at 1.0) for the 1.1 J input pulse while the Monte Carlo/FE models gives an output of 181 at the end of the pulse and 7.9 E+5 after 5 seconds. Since the damage integral integrates the temperature-time history of the temperature increases, the results for the two models can be made equivalent simply by adjusting the input parameters to this damage integral. However the Monte Carlo/FE model does not provide for the different degrees of burn levels as does the Takata Model simply because no levels have been specified for the degrees of burn.

#### 4. DISCUSSION AND CONCLUSION

The original Takata Skin thermal model used by the Air Force for prediction of laser induced damage was flawed by its Beer's Law algorithm for the absorption of light. For visible and near IR wavelengths, the heat source term for thermal models must be modified to incorporate light scattering in tissue. However, near the 1.45  $\mu\text{m}$  water absorption peak,  $\mu_a$  is greater than  $\mu_s$ . At 1315 nm, the ratio between reduced scattering and absorption is slightly larger than 8 to 1. The significance of this scattering in the thermal response is provided by the computed temperature rise for the Beer's Law Model (Takata) and Monte Carlo/FE Model. Comparison between the experimental data obtained from porcine skin at this wavelength and the model predictions resulted in wide discrepancy between predictions and measurements. It is believed that these discrepancies were the result of absorption parameters and spot size input parameters because Takata et al. validated the model<sup>5</sup> with 1.5 cm spot sizes and we were using spot sizes less than 1 mm in diameter

High-speed *in vivo* temperature measurements were taken to provide data for validating these models along with the skin parameter measurements for input requirements to the model. Thus we have much more confidence in our data when the same skin samples were used for both temperature measurements and absorption and scattering parameter measurements within 24 hours. Temperature measurements were taken using the same laser pulse energies and spot sizes that were utilized for the MVL-ED<sub>50</sub> threshold levels. We now have the MVL-ED<sub>50</sub> threshold exposure levels, temperature measurements above and below these threshold exposures, and two model predictions for the temperature increases and damage levels. A thorough analysis of these data and with the new absorption and scattering coefficients as a function of wavelength, will yield modeling capabilities for much of the near-IR spectrum.

For the temperature measurements shown in Figure 3, a good estimate for the temperature rise at the ED<sub>50</sub> threshold of 0.39 J would be 50 °C or 22.5 °C rise above the

skin ambient temperature. These temperatures were recorded at the end of the laser pulse within 0-to-10 ms post exposure. Thus the peak temperature rise would be expected to be slightly higher but not significantly higher. As shown in Figure 3, the Takata Model predicts the temperature to be 58 °C or a rise of 31 °C when using the new skin parameters. The Monte Carlo/FE Model predicts the temperature to be 64 °C for a temperature rise of 37 °C. Thus there is a 6 °C difference between the Takata Model and Monte Carlos Model when using the same parameters and energies. There are several reasons why the calculated temperatures are higher than measured ones and these include the 10-ms uncertainty in starting of the temperature measurements and other parameters input to the models which have unknown origins. Temperatures measured for the 1.3 mm spot size, (Figure 4), were found to be approximately 43 °C for the threshold energy of 1.1 J for the 350 μs pulse width. The temperature rise calculated by the Takata model was 25 °C for a total temperature of 53 °C. The Monte Carlo Model calculated the temperature to be 587 °C for a 30 °C rise above skin ambient. The measured temperature rise was 14 °C while the calculated temperature rises were 25 and 30 °C. Larger differences between measured and calculated temperature rises were found for the larger spot size than for the smaller spot size. At this time we have no explanation for these differences and more data will be required to understand these models.

Both models are shown in Figures 5 and 6 for the top-hat laser profile showing their calculated spatial temperature profiles. Both profiles show very good correlation with only their magnitudes slightly different. The heat source terms were calculated using different methods and different parameters. The Takata Model uses a tissue absorption coefficient and a surface reflection percentage as the light propagates into the tissue while the Monte Carlo Model uses absorption and scattering coefficients in determining the heat source terms. Peak heat source values were calculated as 168 J/cm and 130 J/cm for the Takata and Monte Carlo Models, respectively. This difference between heat source terms account almost entirely for the differences in calculated temperature rises. There is not enough known about each model to draw any conclusion about which is the most correct and which one should be used to predict damage.

The major difference between the parameters measured herein and those measured 30 years ago is that then light scattering within the skin was not understood well and that internal scattered light was considered to be reflected back to the surface and be included within the reflection coefficient. For large spot sizes the Takata Model predicts the temperature rises adequately but breaks down for very small spot sizes. We now know that light is scattered within the tissue and the light transport can be calculated using a scattering coefficient or reduced scattering coefficient<sup>3</sup> within the Monte Carlo/FE Model. Other researchers have reported porcine skin measurements which are similar to our measurements. The main difference between the our measurements and those reported by Du, et al<sup>10</sup> is the facts that our measurements are from a porcine skin containing melanin granules and the UNC came from a white domestic pig with white skin and no melanin. We only used our measured values in the calculations reported herein because the temperature measurements were from a skin with melanin granules.

## 5. REFERENCES

1. American National Standards Institute, *American National Standard for the Safe Use of Lasers*, New York, ANSI Standard Z136.1, 2000
2. J. A. Zuclich, D. A. Gagliano, F. E. Cheney, B. E. Stuck, H. Zwick, P. R. Edsall, and D. J. Lund, *Ocular effects of penetrating IR laser wavelengths*, Proc. SPIE, vol. 2391, pp. 112-125, 1995
3. B. E. Stuck, D. J. Lund, and E. S. Beatrice, *Ocular Effects of Holmium (2.06  $\mu\text{m}$ ) and Erbium (1.54  $\mu\text{m}$ ) Laser Radiation*, Health Physics, vol. 40, pp. pp. 835-846, 1981
4. J. A. Zuclich, H. Zwick, S. T. Schuschereba, B. E. Stuck, and F. E. Cheney, *Ophthalmoscopic and pathologic description of ocular damage induced by infrared laser radiation*, Journal of Laser Applications, vol. 10, pp. 114-120, 1998
5. A. N. Takata, L Zaneveld, and W. Richter, *Laser-Induced Thermal Damage of Skin*, Report SAM-TR-77-38, Brooks Air Force Base, TX Dec. 1977
6. A.J. Welch and M.J.C. van Gemert, Editors, *Optical-Thermal Response of Laser Irradiated Tissue*, Plenum Press, New York, 1995, 78-99
7. T.A. Eggleston, W.P. Roach, M.A. Mitchell, K. Smith, D. Oler and T.E. Johnson, *Comparison of Two Porcine (*Sus scrofa domestica*) Skin Models for In Vivo Near-Infrared Laser Exposure*, Comparative Medicine, Vol. 50, No. 4, 2000
8. D. J. Finney, *Probit Analysis, Third Edition*, Cambridge University Press, London, 1971
9. F.C. Henriques, "Studies of Thermal Injury", *Arch.Pathol.*, vol.43, pp. 489-502, 1947
10. Y. Du, X. H. Hu, M. Cariveau, X. Ma, G. W. Kalmus, and J.Q. Lu, *Optical Properties of porcine skin dermis between 900 nm and 1500 nm*, Phys. Med. Biol. **46**(2001) 167-181.